Nanoscale

Accepted Manuscript

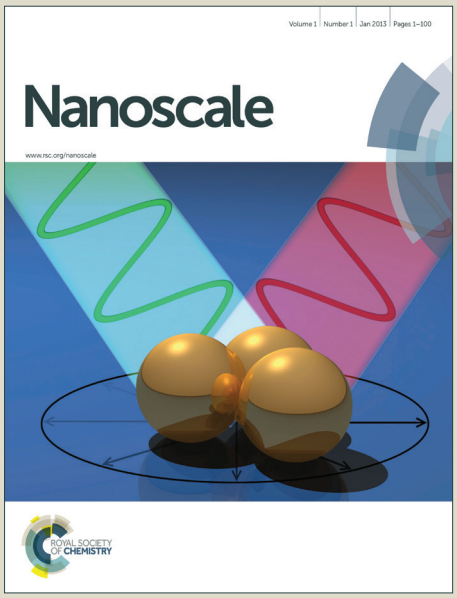

Journal Name
Nanoscale
Dynamic Article Links ►

Cite this: DOI: 10.1039/c0xx00000x

www.rsc.org/xxxxxx

ARTICLE TYPE

Template Engaged Synthesis of Hollow Ceria-Based Composites

Guozhu Chen,[a*] Federico Rosei[b*] and Dongling Ma[b*]

Received (in XXX, XXX) Xth XXXXXXXXX 20XX, Accepted Xth XXXXXXXXX 20XX
DOI: 10.1039/b000000x

Hollow ceria-based composites, which consist of noble metal nanoparticles or metal oxides as a secondary component, are being studied extensively for potential applications in heterogeneous catalysis. This is due to their unique features, which exhibit the advantages of hollow structure (*e.g.* high surface area and low weight), and also integrate the properties of ceria and noble metals/metal oxides. More importantly, the synergistic effect between constituents in hollow ceria-based composites has been demonstrated in various catalytic reactions. In this feature article, we summarize the state-of-the-art in the synthesis of hollow ceria-based composites, including traditional hard-template and more recently, sacrificial-template engaged strategies, highlighting the key role of selected templates in the formation of hollow composites. In addition, the catalytic applications of hollow ceria-based composites are briefly surveyed. Finally, challenges and perspectives on future advances of hollow ceria-based composites are outlined.

1. Introduction

During the past decade, hollow structured nano- and micro-structured materials have attracted increasing attention due to their unique features, such as large surface area, low density, low coefficients of thermal expansion and refractive indices, and good surface permeability for charge and mass (gas) transport, which make them attractive for applications in catalysis, lithium-ion batteries, and drug encapsulation and delivery.[1-15] So far, tremendous advances have been achieved in the synthesis of hollow micro-/nanomaterials by adopting various strategies. Among these synthetic approaches, a hard template-engaged method is being widely used to prepare different hollow architectures.[4,5]. In this method, the whole process normally involves (i) the selection and preparation of templates, (ii) coating the templates with desired materials or their precursors, possibly followed by a post-treatment to form a core@shell structure, (iii) removal of core templates by calcination or wet chemical etching. Silica particles, polymer latex colloids, and carbon spheres are the most commonly employed hard templates (termed as conventional hard templates to distinguish them from sacrificial templates hereafter). In using such conventional hard templates, functionalization/modification of the template surface may be a necessary step to overcome the incompatibility between template surface and shell materials, to avoid the homogeneous nucleation of shell materials in solution.[4] When hard templates themselves are involved as precursors in the synthetic process of shell materials, they are named "sacrificial templates". Sacrificial template synthesis is inherently advantageous because surface functionalization/modification is unnecessary in this case and the shell material deposition onto the template is guaranteed through a chemical reaction. It has already been amply demonstrated that the formation of a hollow structure is largely dependent on the physico/chemical properties of sacrificial templates such as standard reduction potential, solubility product constants (K_{sp}), and diffusion rates.[16-26] The selection of suitable sacrificial templates is therefore an essential prerequisite for the synthesis of desired hollow structures.

Ceria is considered as one of the most important components in many catalytic systems because it can act as an oxygen buffer by releasing/uptaking oxygen through redox processes involving the Ce^{4+}/Ce^{3+} couple. Of particular interest is that a strong synergistic effect can potentially be observed in catalytic reactions when ceria is combined with noble metals or other low-cost transition-metal oxides to form ceria-based composites.[27-39] For example, cationic gold species can strongly bind to the oxygen vacancies of ceria and thus be stabilized. Together with the introduction of electronic effects between gold and ceria, they have been proposed to be responsible for the improved catalytic activity demonstrated in CO oxidation.[40-43] In the case of ceria-based binary metal oxide, foreign cations (*e.g.* Co) may modify the surface oxygen vacancies of ceria at the atomic level, promoting a remarkable increase in the oxygen storage capacity of ceria nanoparticles (NPs).[35]

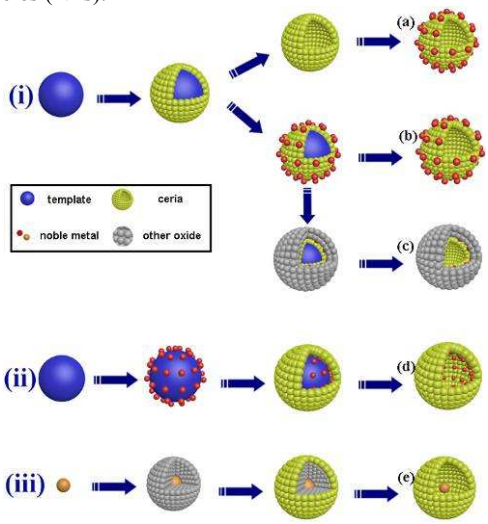

Scheme 1 Various synthetic strategies of hollow ceria-noble metal NP composites.

To optimize the synergistic interaction between ceria and integrated secondary species, many strategies have been attempted. For example, hollow ceria-noble metal NP composites were designed and realized in different configurations, including

Templates	Composites	Preparation Process	Notes	Reference
Carbon spheres	CeO_2-Au	Adsorption and penetration of Ce^{3+} ; Removal of carbon template; Deposition of Au NPs on the mutil-shelled CeO_2	The increase of contact surface between Au and CeO_2, leading to high activity in the reduction of 4-NP	[44]
Carbon spheres	CeO_2-Pd	Deposition of Pd NPs on the carbon spheres; Growth of CeO_2 shell; Removal of carbon template	Aggregation- and leaching-resistant of Pd NPs; Efficient catalyst for thermo- and photo-catalytic selective reduction of aromatic nitro compounds	[62]
Silica spheres	CeO_2/M (M=Au, Pd, AuPd)	Deposition of NPs on the silica spheres; Mixing with CeO_2 sol to get CeO_2 shell; Removal of silica template	Hollow, mesoporous structured CeO_2 and synergistic effect, leading to high activity in the reduction of 4-NP	[61]
Silica spheres	Au-CeO_2-Pd-TiO_2	Growth of CeO_2 shell on the silica spheres; Removal of silica template; Deposition of Au NPs on the CeO_2 surface; Continued growth of silica shell; Deposition of Pd NPs and growth of TiO_2 shell; Removal of silica	Multiple interactions and strong synergistic effect, leading to high activity in the Suzuki–Miyaura coupling reaction, benzyl aerobic alcohol oxidation and 4-NP reduction reaction	[46]
Silica particles	CeO_2-Pt	Deposition of Fe_2O_3 on the Pt NPs; Coating silica; Removal of Fe_2O_3; Growth of CeO_2 shell; Removal of silica	Multi-york-shell structured catalyt; High activity towards the CO oxidation; High thermal stability	[51]
Mesoporous silica	CeO_2-M (M=Au, Pt, Pd)	Impregnation with Ce salts; Calcination and removal of silica; Impregnation with Pt salt; Calcination and reduction	NPs encapsulated in channels of mesoporous CeO_2; High concentration of oxygen vacancies in the internal concave surface of CeO_2, resulting in low activiation energy in WGS reaction	[47]
Mesoporous silica	CeO_2-Pt	Impregnation with Ce salts; Calcination and removal of silica; Deposition of Pt NPs	The charger transfer at the Pt-CeO_2 interface, resposible for the high CO oxdidation rate	[48]
Polystyrene fibers	CeO_2-Pt	Deposition of Pt NPs on the polystrene fibers; Growth of CeO_2 shell; Removal of polystyrene fibers	Pt NPs embedded in the inner surface of CeO_2; Sinter-resistant catalyst; High catalytic activity in CO oxidation	[63]
Alumina membranes	Ce-Co mixed oxide	Deposition of Ce-Co mixed oxide on the alumina membrane by means of electrochemical method, followed by removal of template	Tunable compositions	[67]
Polycarbonate membrane	Ce-Zr mixed oxide	Dehydration and denitrification of mixed metal precursors, followed by removal of template	Different CeO_2% NTs having different structures (cubic or tetragonal phase)	[68]
Polystyrene spheres	Ce-Sn mixed oxide	Coating $Ce(OH)_3$-$Sn(OH)_4$ on the polystyrene; Calcination	Ce-doped SnO_2; perfect sensing performance toward acetone gas with rapid response, good stability and high temperature response	[71]
$Ce(OH)CO_3$ nanorods	CeO_2-Au	Preparation of CeO_2 NTs; Deposition of Au NPs	Au NPs prepared by laser-ablation method; Strong interaction between Au NPs and CeO_2; High activity in CO oxidation and the reduction of 4-NP	[45]
$Ce(OH)CO_3$ nanorods	CeO_2-Au	Au(III) reduced by Ce(III); Ce(III) oxidized to Ce(IV); Hydrolysis of Ce(IV)	Au@CeO_2 core-shell NPs supported on CeO_2 NTs; Thermal stability; High activity in CO oxidation	[77] [73]
Ag nanowires	CeO_2-Ag	Coating CeO_2 on Ag nanowires; Partial Ag atom migration outward	The Ag doped CeO_2 NTs formed by Kirkendall diffusion	[6]
Cu_2O cubes	Ce-Cu mixed oxide	Partial Cu_2O etching due to redox reaction between Cu_2O and Ce(IV); Hydrolysis of Ce(IV)	Ce-Cu mixed oxides prepared from cubic and octahedral Cu_2O templates exhibit different compositions and structures	[74]
$Ce(OH)CO_3$ nanorods	Ce-Mn mixed oxie Ce-Fe mixed oxide	Redox reaction between $Ce(OH)CO_3$ and MnO_4^- / FeO_4^{2-} Hydrolysis of Ce(IV) and removal of template	Close contact between CeO_2 and MnO_2; Synergistic effect between Ce and Mn in CO oxidation	[78]

Tab.1 Summary of the hollow ceria-based composites prepared from template-engaged methods. Templates presented in the upper part are hard templates and those shown in the lower part are sacrificial templates.

noble metal NPs supported on the external surface of hollow ceria (Scheme 1 (i)), anchorage of NPs onto the inner surface of ceria (Scheme 1 (ii)) and encapsulation of NPs by ceria to form the so-called yolk shell structure (Scheme 1 (iii)).[44-51] Most of them exhibited remarkable catalytic properties because these kinds of structures could either avoid the migration and aggregation of noble metal NPs at high temperature or optimize the fraction of the interfacial area of the two components in the composites. Although there are many successful examples in synthesizing hollow ceria nanomaterials, significant challenges, such as the selection of appropriate templates, and relevant template surface modification to avoid homogeneous nucleation of the involved secondary species, still need to be addressed towards the

controlled synthesis of such composites.

Herein, we highlight recent advances in the synthesis of hollow ceria-based composites, as summarized in Table 1, primarily focusing on template-engaged synthetic strategies. In the first section, we start by using the conventional hard template approach for the synthesis of hollow ceria-based composites. Next, we demonstrate that hollow ceria-based composites can be prepared by means of the sacrificial template approach. In addition, the catalytic performances of the ceria-based composites are also summarized. Finally, remarks on promising opportunities and relevant challenges regarding the synthesis and fundamental understanding of such systems are also discussed.

2. Conventional hard-template approach to synthesize hollow ceria-based composites

2.1. Hollow ceria-noble metal composites

The conventional hard-template assisted approach represents a straightforward and powerful route towards the synthesis of nanostructures with hollow interiors. The template simply serves as a structural scaffold, around which the desired shell material is generated *in situ* and directed to grow into a nanostructure with its morphology complementary to that of the template. The hard template is subsequently removed by calcination at high temperature or by dissolution via chemical etching.[4,5] Until now, different hollow structured pure ceria has been prepared with the assistance of conventional hard templates.[52-60] These hard templates can also be used to synthesize hollow ceria-based composites.

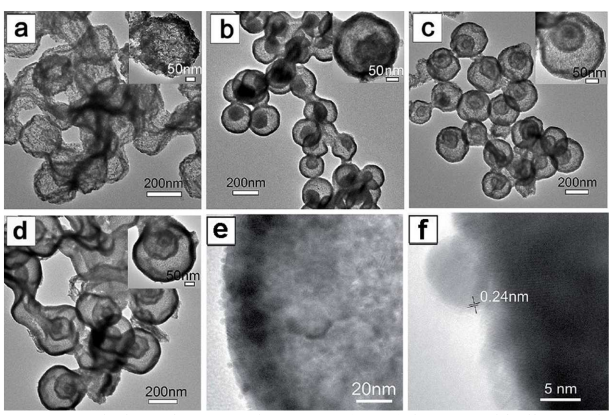

Fig. 1 Transmission Electron Microscopy (TEM) images of hollow ceria nanospheres with various shell numbers obtained at different heat ramp rates: (a) single shell, (b) double shell, (c) triple shell, (d) quadruple shell, and (e-f) TEM images of triple shell ceria loaded with Au NPs. Reprinted with permission from Ref.44. Copyright 2014 Royal Society of Chemistry.

For hollow ceria-noble metal composites, metal NPs can be either supported on the external surface or encapsulated in the interior space of the hollow ceria. In the first case, hollow ceria nanomaterials are normally pre-synthesized by removing the hard templates, followed by the deposition of noble metal NPs. For example, due to rich surface hydrophilic functional groups (-OH and -COOH), good affinity with Ce^{3+} ions and accessible pore channels, carbonaceous microspheres were used as conventional hard templates for the synthesis of hollow ceria.[44] After controlled calcination with appropriate heat ramp rates of 1 ^{o}C/min, 2 ^{o}C/min, and 10 ^{o}C/min, single-, double-, triple-, and even quadruple-shell hollow ceria nanospheres were successfully obtained. The formation of these different hollow ceria structures was due to the redistribution and penetration of cerium species during calcination. Increasing the heat ramp rate facilitated the spreading of the cerium species in the spheres before causing any combustion of the organic species, leading to deeper penetration of the cerium species and finally more shells. Moreover, Au NPs prepared by $NaBH_4$ reduction of $HAuCl_4$ with sizes below 5 nm were effectively deposited and well dispersed on the synthesized multi-shelled ceria (Fig. 1 and (a) in Scheme 1).[44] Recently, Zhang *et al.* used silica as a hard template to synthesize hollow ceria, then loaded Au NPs onto the ceria surface.[46] Using the obtained hollow ceria-Au composite as a substrate, they further coated it with silica, Pd NPs, and TiO_2 via a layer-by-layer deposition process. After the removal of silica with an alkali etching method, double shelled CeO_2@M@M@TiO_2 (M=Au and/or Pd) nanospheres with dual noble metal NPs encapsulated in metal oxide shells were achieved ((c) in Scheme 1).[46] Under a similar mechanism, ceria/noble metal composites were formed when the ceria sol was mixed with pre-synthesized noble metal NP-silica composites, followed by removal of templates ((b) in Scheme 1).[61] In addition, mesoporous ceria was often prepared from mesoporous silica templates through calcination of impregnated cerium salts and subsequent removal of silica. The ceria-noble metal NP composites can then be achieved by mixing porous ceria with pre-synthesized NPs or impregnation of noble metal salt solutions followed by calcination.[47, 48]

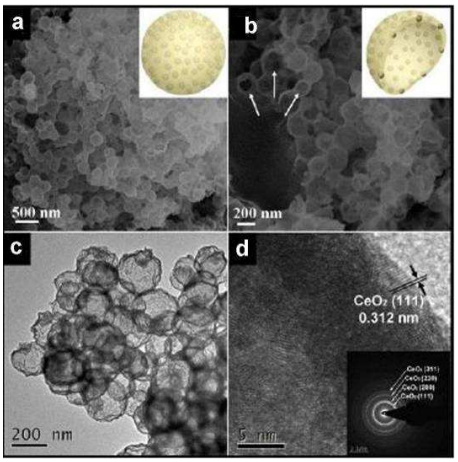

Fig. 2 Typical (a, b) scanning electron microscope (SEM), (c) TEM, and (d) High resolution-TEM images of Pd@hollow CeO_2 core@shell nanocomposite (the insets of a and b are the corresponding model illustrations; the inset of d is the Selected Area Electron Diffraction (SAED) pattern). Adapted from Ref. 62. Copyright 2013 American Chemical Society.

In contrast, in the latter case, noble metal NPs can be deposited on the surface of selected hard templates first, followed by the coating of ceria. Subsequently the noble metal NPs are encapsulated in the interior space of hollow ceria after the removal of hard templates ((d) in Scheme 1).[62-63] For example, polyvinylpyrrolidone (PVP) stabilized Pd NPs were found to be preferentially loaded onto the surface of carbon spheres to develop into carbon sphere-Pd composites.[62] Since the as-formed composites have negative surface charges, Ce^{3+} adsorbed onto their surface via electrostatic interactions, resulting in the uniform coating of ceria after hydrothermal treatment. After calcination, a Pd@ceria core@shell hollow nanocomposite composed of Pd NP cores 1~5 nm in size encapsulated within the ceria shell was obtained (Fig. 2).[62] Xia *et al.* employed plasma treated polystyrene (PS) fibers as hard templates, and found that the hydrophilic surface of treated PS favored the deposition of PVP-capped Pt NPs.[63] The authors proposed that the Ce^{3+} cations

could easily adsorb onto the Pt NPs to facilitate the nucleation and growth of ceria nanocrystals due to the electrostatic interaction between Ce^{3+} and negatively charged Pt NPs. After the removal of the PS fibers by calcination in air at 400 °C, Pt NPs were successfully embedded in ceria hollow fibers (Fig. 3). Remarkably, due to an effective metal-support contact, the generated catalyst could resist thermal sintering of the Pt NPs up to 700 °C (Fig. 4).[63]

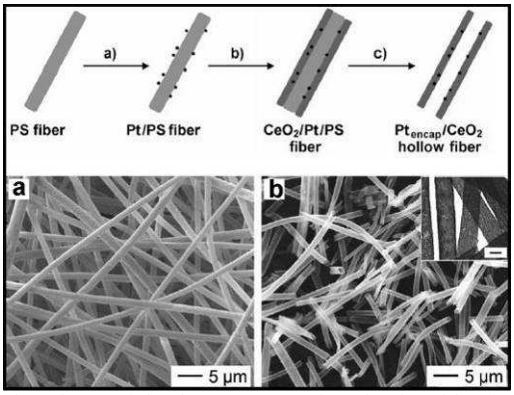

Fig. 3 The scheme of the three-step procedure developed herein for the preparation of ceria-Pt hollow fibers with open ends. SEM images of PS fibers with surfaces that have been coated with Pt NPs and then ceria sheaths before (a) and (b) after calcination (Inset: TEM image confirming the hollow structure; scale bar: 1 μm). Adapted from Ref. 63. Copyright 2012 Wiley-VCH Verlag.

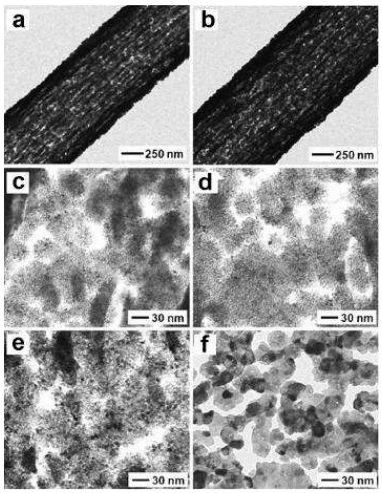

Fig. 4 (a, b) Low-magnification TEM images showing a ceria-Pt hollow fiber after it was calcinated in air for 2 hr at a) 400 and b) 800 °C. c)-f) High-magnification TEM images revealing the wall structures of the ceria-Pt hollow fibers after calcination in air for 2 h at c) 400, d) 600, e) 700, and f) 800 °C. Adapted from Ref. 63. Copyright 2012 Wiley-VCH Verlag.

Alternatively, to achieve noble metal NPs confined in the interior space of the hollow ceria ((e) in Scheme 1), Zheng's group first synthesized hydrophobic Pd NPs, followed by the deposition of Fe_2O_3. Then they coated pre-synthesized Pd-Fe_2O_3 NPs with silica to yield Pd-Fe_2O_3@SiO_2 core@shell NPs. After the removal of Fe_2O_3 by acid, the obtained Pd@SiO_2 core@shell particles reacted with $Ce(NO_3)_3$ to produce Pd@SiO_2@CeO_2 nanospheres. After dissolving the intermediary silica, a "yolk@shell" Pd@CeO_2 structure was obtained.[51] When only hydrophobic Pd NPs without deposited Fe_2O_3 were attempted, it was challenging to uniformly coat silica on their surface due to the tight binding of hydrophobic ligands on the Pd NP surface. Fortunately, hydrophobic Fe_2O_3 can grow epitaxially on Pd. Thus, the presence of Fe_2O_3 on the surface of the Pd NPs was proposed to be a medium that facilitated the encapsulation of the hydrophobic Pd NPs by silica (Fig. 5).[51]

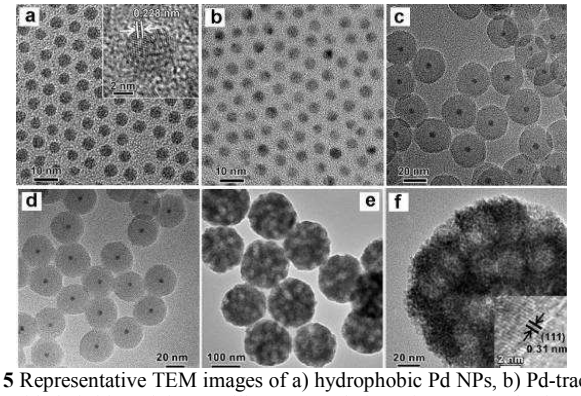

Fig. 5 Representative TEM images of a) hydrophobic Pd NPs, b) Pd-trace iron oxide hybrid particles, c) silica encapsulation of as-prepared Pd-trace iron oxide hybrid NPs, d) Pd@SiO_2, e) hollow Pd@CeO_2 (low-magnification), f) hollow Pd@CeO_2 (high-magnification; inset: typical high resolution-TEM image of the CeO_2 shell). Adapted from Ref. 51. Copyright 2012 Wiley-VCH Verlag.

2.2. Hollow ceria/metal oxide composites

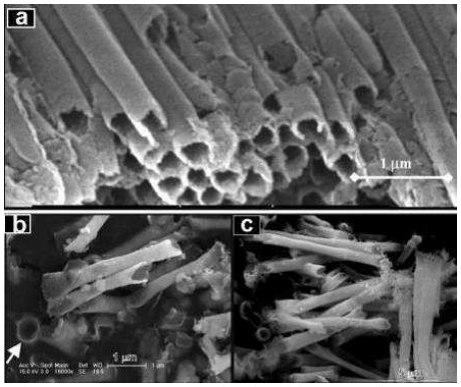

Fig. 6 SEM images of: a) Ce-Co mixed oxide NTs using AAM template, (Adapted from Ref. 67. Copyright 2008. Electrochemical Society) b) $Ce_{0.5}Zr_{0.5}O_2$, and c) $Ce_{0.7}Zr_{0.3}O_2$ NTs using polycarbonate membrane as template (Adapted from Ref. 68. Copyright 2008. American Chemical Society).

Unlike the synthetic process of ceria-noble metal composites, in which ceria and noble metals are normally separately prepared because their synthetic strategies are different, the preparation of ceria-metal oxide composites can be accomplished in one step. In this case, cerium and secondary metal precursors synchronously mix with the employed templates to prepare hollow ceria-metal oxide composites once the templates are removed.[64-70] For example, Ce-Co mixed oxide nanotubes (NTs) were successfully prepared at room temperature by an anodic alumina membrane (AAM) template-engaged process via electrodeposition.[67] In this electrochemical synthesis, the cathodic reduction of Ce-Co mixed nitrate solution and the generation of OH^- ions resulted in the synthesis and deposition of Ce-Co hydroxides on AAM (Fig. 6a).[67] In another scenario, Fuentes *et al*. selected a commercial polycarbonate membrane as a template to fabricate CeO_2-ZrO_2 mixed NTs.[68] The whole preparation process involved the dehydration and denitrification of the confined Ce-Zr precursors in the pores of polycarbonate membrane, and heat treatment to

burn off the templates (Fig. 6 b, c).[68] The Ce-doped SnO_2 hollow spheres were also prepared by the uniform coating of Ce and Sn mixed precursors onto PS spheres, followed by heat treatment at 550 °C to remove the PS templates.[71] Besides these conventional hard templates, Xie *et al*. recently synthesized amorphous Zn-citrate hollow microspheres as starting templates as well as precursors to produce CeO_2-ZnO composites.[65] The -OH and –COO– functional groups present on the surfaces of the Zn-citrate hollow microspheres facilitates the adsorption of Ce^{3+} ions onto their surface. Upon calcination, hollow CeO_2-ZnO composite microspheres were harvested (Fig. 7).[65] In addition, CeO_2-In_2O_3 NTs were fabricated by electrospinning method, where Ce and In nitrate salts were mixed with PVP to form a polymer composite solution, followed by electrospinning and annealing.[69] The electrospinning method is an efficient and general approach to synthesize bimetal oxide NTs, although it hardly falls within the scope of the present article and will therefore not be discussed extensively.[69]

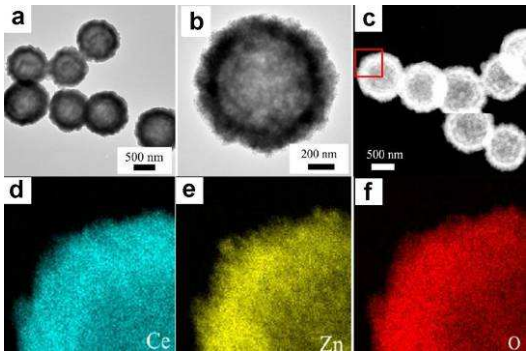

Fig. 7 The low- (a) and high- (b) magnification TEM images of hollow CeO_2-ZnO composites. (c) High Angle Annular Dark Field (HAADF) image of hollow CeO_2-ZnO composite. Elemental mappings of Ce (d), Zn (e), and O (f) obtained from the square region in part c. Adapted from Ref. 65. Copyright 2014 American Chemical Society.

3. Sacrificial-template approach to synthesize hollow ceria-based composites

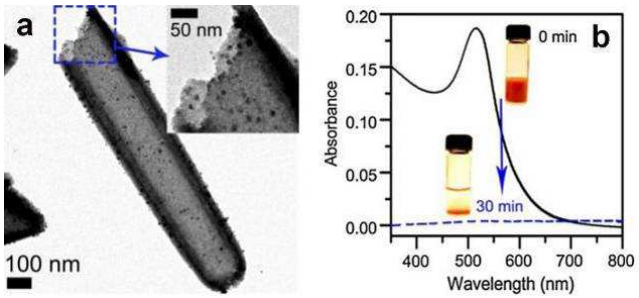

Fig. 8 TEM images of (a) laser ablated Au NP-CeO_2 NT composite. Inset is the magnified TEM image. (b) UV-Vis spectra of laser ablated Au NP solution at 0 min (solid line) and 30 min (dash line) after the addition of CeO_2 NTs. Adapted from Ref. 45. Copyright 2012 Elsevier B.V.

As stated above, sacrificial templates participate in the chemical reaction during the synthesis of hollow materials. The involved reactions mainly consist of ion exchange reactions and redox reactions, which have been used to describe the hollow structure formation mechanisms, such as the Kirkendall effect and galvanic replacement. In a Kirkendall diffusion system, the difference in diffusion rates of different species across an interface in opposite directions results in a net flow of matter, which is balanced by an opposite flow of vacancies. The hollow structure is then formed upon the aggregation of these vacancies. As for the galvanic replacement approach, it is essentially an electrochemical process that requires different reduction potentials for ions in templates and in solution. For example, cerium(III)-containing templates, such as $Ce(OH)_3$ and $Ce(OH)CO_3$, where the Ce(III) ions have a lower reduction potential, can reduce noble metal ions to metals, or reduce metal-containing anions (*e.g.* MnO_4^-, FeO_4^{2-}) to metal oxides. Similarly, a redox reaction between secondary species-containing templates (*e.g.* Cu_2O) with Ce(IV) ions results in ceria-based composites.[72-78]

3.1. Hollow ceria-noble metal composites

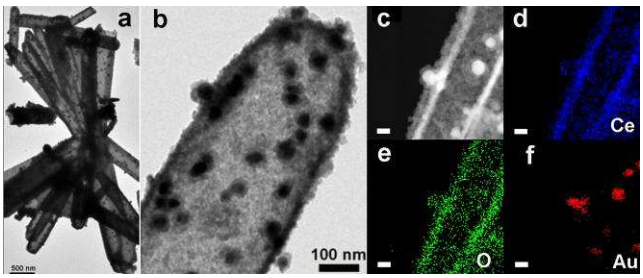

Fig. 9 TEM images (a,b) and HAADF image (c) of the CeO_2-Au nanocomposite, and selected HAADF-STEM image (c) and Ce (blue), O (green), and Au (red) STEM-EDS maps (d-f). Scale bar: 20 nm. Adapted from Ref. 77. Copyright 2013 Royal Society of Chemistry.

Similar to the conventional hard-template approach, hollow ceria/noble metal composites can be prepared by loading Au NPs onto pre-synthesized hollow ceria derived from cerium-containing sacrificial template. For example, three types of ceria NTs were fabricated through interfacial reaction between $Ce(OH)CO_3$ and NaOH. In this solid-liquid reaction system, $Ce(OH)CO_3$ nanorods acted as sacrificial template, providing Ce^{3+} to react with OH^-. Thus, the formed $Ce(OH)_3$ shell deposited on the external surfaces of $Ce(OH)CO_3$ nanorods. Since $Ce(OH)_3$ is easily oxidized into $Ce(OH)_4$, which can be dehydrated and converted into CeO_2 during the drying process, the ceria NTs can be obtained after removing residual $Ce(OH)CO_3$.[79,80] For example, ceria-Au composites were fabricated using these as-synthesized ceria NTs by simply mixing them with laser ablated Au colloids, which showed very efficient anchorage, as reflected from the dramatic decrease of Au surface plasmon resonance measured from solution (Fig. 8).[45] Considering the reduction ability of Ce (III), these highly interesting $Ce(OH)CO_3$ nanorod templates can be further employed in the oxidation-reduction reactions with oxidizing agents to directly form nanocomposite structures. Chen *et al*. developed a simple method for direct synthesis of Au@CeO_2 core@shell structured NP-CeO_2 NT composite by mixing $HAuCl_4$ and $Ce(OH)CO_3$ nanorods under mild conditions (Fig. 9).[77] The formation of ceria-Au composite was due to the interfacial oxidation-reduction reaction between $HAuCl_4$ and $Ce(OH)CO_3$, where Au (III) in $HAuCl_4$ was reduced to Au (0) by Ce (III) in $Ce(OH)CO_3$, while Ce (III) was oxidized into Ce(IV), followed by hydrolysis to generate ceria. The slow hydrolysis rate of Ce(IV) led to the coverage of ceria on the Au NPs, and on the residual $Ce(OH)CO_3$ surface, developing into Au@CeO_2 and $Ce(OH)CO_3$@CeO_2 core@shell structures. Further depletion/dissolution of $Ce(OH)CO_3$ eventually resulted in Au@CeO_2 core@shell NP-CeO_2 NT composite. The advantages of this synthetic strategy are that it is independent of foreign reducing agents and additional surface modification. Moreover, such core@shell NP-NT composite can be obtained in one step, simplifying the synthesis procedures greatly (Scheme 2).[77] Recently, Yang *et al*. used a similar method to synthesize Au NP-

decorated $Gd_{0.3}Ce_{0.7}O_{1.9}$ NTs by selecting $Gd_{0.3}Ce_{0.7}(OH)CO_3$ as a sacrificial template.[73]

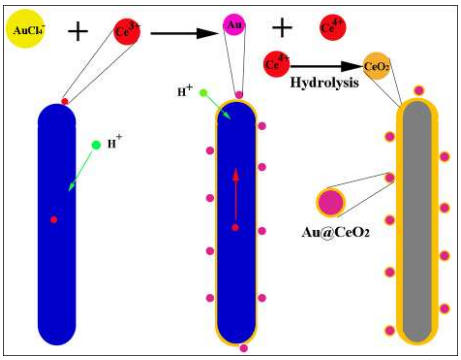

Scheme 2 Schematic illustration for the formation of Au@CeO_2 core@shell NP-CeO_2 NT nanocomposite. Adapted from Ref. 77. Copyright 2013 Royal Society of Chemistry.

In addition to cerium-containing precursors, metals can also act as templates to synthesize hollow ceria-metal composites. For example, Mendoza-Anaya selected Ag nanowires as template to synthesize Ag NP-CeO_2 NT composites.[6] During the synthetic process, CeO_2 NPs first covered the Ag nanowires. As the reaction proceeds, a fraction of the Ag nanowires reacted with ammonium hydroxide introduced to the reaction solution, and Ag atoms migrated outside. When the sintering process was applied, out-diffusion of the remnant Ag through the interface was faster than the in-diffusion of the ceria shell material, which eventually resulted in a hollow Ag-CeO_2 composite (Fig. 10).[6]

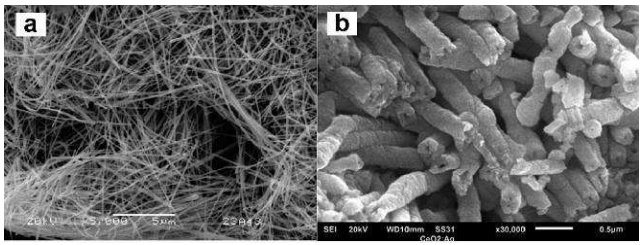

Fig. 10. SEM images of a) Ag nanowires used as templates, b) Ag-CeO_2 tubular structure. Reprinted with permission from Ref.6. Copyright 2011 Royal Society of Chemistry.

3.2. Hollow ceria-metal oxide composites

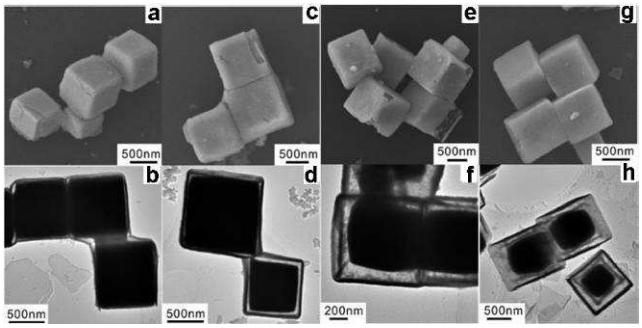

Fig.11 SEM and TEM images of different compositions of hollow CeO_2-Cu_2O composites when Cu_2O cubes were employed as sacrificial templates. Adapted from Ref. 74. Copyright 2014 American Chemical Society.

When a Ce(IV)-containing species is employed as a precursor, it may react with some metal oxides with a certain reduction ability to form ceria-metal oxide composites. For example, Cu_2O, a widely used sacrificial template, could react with $(NH_4)_2Ce(NO_3)_6$ ethanol solution by a liquid (Ce(IV))−solid (Cu_2O) interfacial redox reaction.[74] Hollow CeO_2-CuO composites were achieved when a large amount of Ce(IV) precursor was used (Fig. 11). The authors proposed that the etching of Cu_2O nanocrystals was initiated by the redox reaction between Cu_2O and Ce(IV). The produced OH^- would dominantly combine with Ce^{4+} since the solubility product constant (K_{sp}) of $Ce(OH)_4$ ($K_{sp} = 2 \times 10^{-48}$) is significantly smaller than that of $Ce(OH)_3$ ($K_{sp} = 1.6 \times 10^{-20}$) and $Cu(OH)_2$ ($K_{sp} = 2.2 \times 10^{-20}$). Thus, CuO formed only in the presence of a large amount of Ce(IV), simultaneously producing high concentrations of OH^-.[74] Another interesting approach is to use an acidic $Ce(NO_3)_3$ solution to etch ZnO templates to obtain ceria NTs.[81] The release of H^+ accompanied with the precipitation of ceria after the hydrolysis of Ce(III) resulted in an instantaneous dissolution of the ZnO templates. When the sacrificial ZnO templates were not completely dissolved by H^+, a hollow ceria-ZnO composite was achieved instead.[81] In addition, ceria, which can act as both a chemical (reactive) and physical (non-reactive) template, was employed to prepare hollow ceria-ZrO_2 nanocages by Li *et al.*[75] In this case, the pre-synthesized ceria clusters had high reactivity and diffusion rates due to the presence of secondary structures. Thus, Zr^{4+} could readily dope into ceria to form the solid solution of $Ce_{1-x}Zr_xO_2$. As the secondary nanostructure of pre-synthesized ceria clusters diffused faster to the outside than the inward diffusion of Zr^{4+}, the hollow ceria-ZrO_2 nanocages were eventually developed using the Kirkendall effect (Fig. 12).[75]

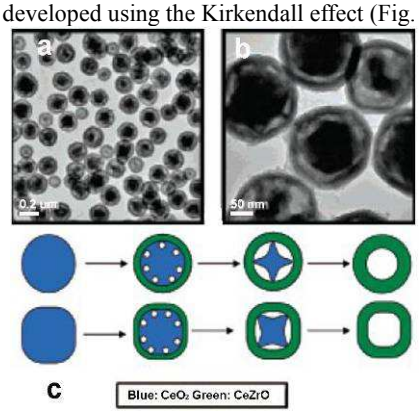

Fig. 12 (a-b) Typical TEM images with different magnifications of the hollow core@shell nanostructures obtained by shortening the reaction time; (c) the illustration about the formation process of the Ce-Zr-O nanocages based on the Kirkendall effect. Adapted from Ref. 75. Copyright 2014 American Chemical Society.

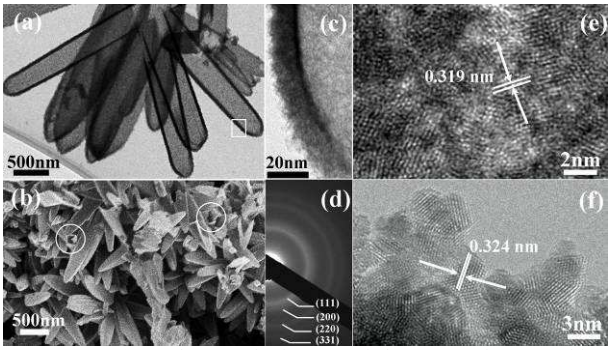

Fig. 13 TEM (a) and SEM (b) images of the prepared Ce-Mn binary oxide NTs without heat treatment; (c) magnified TEM image of the rectangle part in (a); SAED pattern (d); High resolution-TEM images of the inner surface (e) and the outer surface (f) of the heat-treated NTs. Adapted from Ref. 78. Copyright 2012 Wiley-VCH Verlag.

Since Ce has two oxidation states, Ce(III) and Ce(IV), it is possible to synthesize ceria-metal oxide composites by choosing Ce(III)/Ce(IV) precursors to perform an oxidation/reduction reaction with certain oxidizing/reducing agents. For example, when a $Ce(OH)CO_3$ template was mixed with $KMnO_4$ aqueous solution, MnO_4^- was reduced to manganese oxide and the Ce^{3+} in $Ce(OH)CO_3$ was simultaneously oxidized to form ceria. After selective removal of the residual template with acid, Ce-Mn binary oxide NTs were obtained (Fig. 13).[78] From the HAADF-STEM image and elemental maps, Ce, Mn and O were uniformly distributed in the wall of this representative NT. Such uniform distribution of Ce and Mn is beneficial to strengthen their interaction in the binary oxide (Fig. 14). More importantly, hollow Ce-Mn binary oxide cubes, and Co-Mn and Ce-Fe binary oxide hollow nanostructures could all be achieved by this method by changing the shape of the $Ce(OH)CO_3$ templates from rods to cubes, changing the templates from $Ce(OH)CO_3$ nanorods to $Co(CO_3)_{0.35}Cl_{0.20}(OH)_{1.10}$ nanowires, or replacing the oxidant of $KMnO_4$ with another strong one, K_2FeO_4, respectively (Fig. 15).[78]

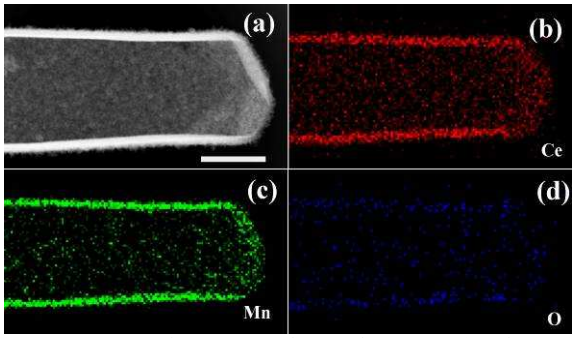

Fig. 14 HAADF-STEM image (a), and Ce-L (b), Mn-K (c) and O-K (d) STEM-EDX maps of an individual NT after heat treatment. Scale bar: 200 nm. Adapted from Ref. 78. Copyright 2012 Wiley-VCH Verlag.

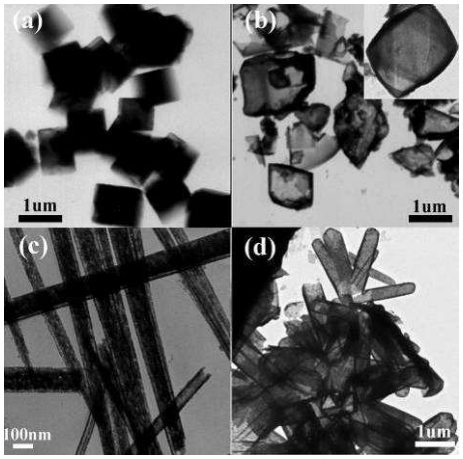

Fig. 15 TEM images of (a) $Ce(OH)CO_3$ cube templates and (b) as-prepared hollow Ce-Mn binary oxide cubes without further heat-treatment. (c) Co-Mn binary oxide and (d) Ce-Fe binary oxide hollow structures. Inset in (b) is a magnified hollow cube. Adapted from Ref. 78. Copyright 2012 Wiley-VCH Verlag.

From the examples above, $Ce(OH)CO_3$ was demonstrated as a good sacrificial template in the synthesis of hollow ceria-based composites, because (1) Ce(III) having certain reduction ability enables the reduction of $HAuCl_4$ and $KMnO_4$; (2) the as-formed Ce(IV) ions easily undergo hydrolysis to produce ceria, which preferentially deposits on the $Ce(OH)CO_3$ template surface; (3) $Ce(OH)CO_3$ can be dissolved by acid while ceria cannot, which is the prerequisite for the formation of a hollow structure (Scheme 3).

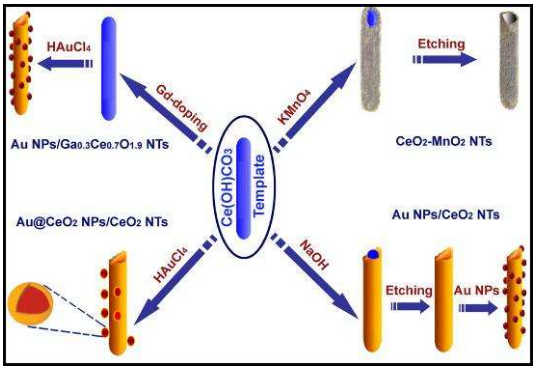

Scheme 3 A schematic illustration of the $Ce(OH)CO_3$ nanorods as sacrificial templates to synthesize ceria-based hollow composites.

4. Catalytic performance of hollow ceria-based composites

It has been well documented that the interactions between secondary noble metal NPs (or metal oxides) and ceria endow ceria-based composites with high catalytic activity in certain reactions.[82-85] Herein, we discuss the catalytic performance of the ceria-based composites in terms of activity, thermal stability and reproducibility based on a series of model reactions, such as carbon monoxide oxidation, 4-nitrophenol reduction, and alcohol oxidation. The structure-activity relationship is also briefly discussed.

4.1 Hollow ceria-noble metal composites

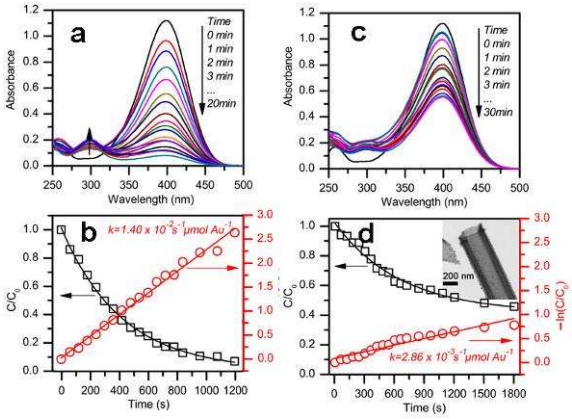

Fig. 16 UV-Vis absorption spectra during the catalytic reduction of 4-nitrophenol over laser ablated Au NP-CeO_2 NT (a) and chemical prepared Au NP-CeO_2 NT composites (c); C/C_0 and $-\ln(C/C_0)$ as a function of reaction time for the reduction of 4-nitrophenol over laser ablated AuNP-CeO_2 NT (b) and chemical prepared Au NP-CeO_2 NT (d) composites. Adapted from Ref. 45. Copyright 2012 Elsevier B.V.

Since noble metal NPs have high surface energy, they tend to migrate and sinter into larger particles during catalytic reactions, resulting in deterioration of catalytic activities.[51] Therefore, the role of hollow ceria as support is primarily to stabilize noble metal NPs to prevent their sintering during catalytic reactions. In addition, ceria also works as an electronic modulator for the loaded noble metal NPs. For example, the composite made of ceria NTs and Au NPs, synthesized by laser ablation, exhibited

superior catalytic performance towards the reduction of 4-nitrophenol in comparison to chemically synthesized Au NPs (Fig. 16).[45] Since there are no surfactants on the laser-prepared Au NPs, the ceria NTs coupled directly with these Au NPs without suffering from any steric hindrance, resulting in a stronger interaction at the ceria-Au interface. It was proposed that the interaction between ceria and Au may accelerate the electron transfer from BH_4^- to 4-NP in the hydrogenation process, leading to the superior catalytic performance in the reduction of 4-nitrophenol.[45] For those catalytic reactions carried out at high temperature, the deposition of noble metal NPs on the outer surface of hollow ceria cannot completely prevent their migration and sintering. Nonetheless, the encapsulation of noble metal NPs into hollow ceria may effectively delay the undesirable aggregation of the NPs because of the largely decreased mobility of the NPs due to the limited space inside the hollow ceria, thus significantly improving catalytic stability. For example, a hollow and mesoporous ceria-Pd composite displayed a much higher catalytic activity (Fig. 17) as well as remarkably enhanced stability due to the considerable promoting effect of ceria on the Pd NPs.[51] No loss in the catalytic activity was observed even for the mesoporous ceria-Pd composite treated at 550°C for a period of six hours in the aerobic selective oxidation of cinnamyl alcohol to cinnamaldehyde (Table 2).[51] Similarly, the ceria layer on Pt was suggested to accelerate the overall reaction rate of CO oxidation by participating in accepting and donating oxygen atoms, which compensated the limited accessibility of reactants to the catalytic sites.[35] For more complex structures, such as double shelled hollow ceria with dual noble metal NPs encapsulation, Zhang *et al.* proposed three key factors that are responsible for their high catalytic activity toward CO oxidation.[46] First, the interspaces between the double shells can form a microreactor that confines the reactants, providing a driving force to accelerate the catalytic reaction. Second, as the active species are distributed in both the external and internal surface, the unique double-shelled structure can increase the number of active sites in the microreactor and improve the contact of active species with reactants, favoring the improvement of catalytic performance. Third, the double shelled structure can create double noble metal–metal oxide interfaces, which may enhance the synergistic effect of noble metal NPs with oxide supports, thus leading to the improvement of catalytic performance.[46]

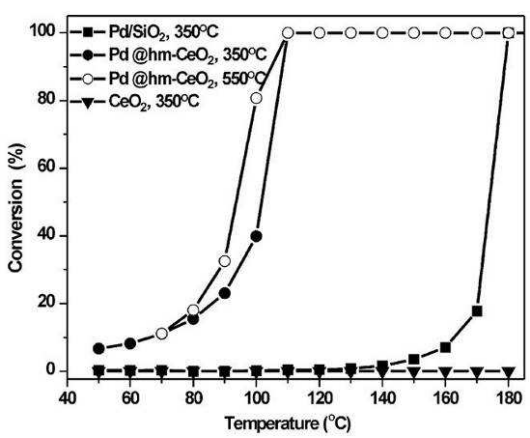

Fig. 17 CO oxidation conversion light-off curves of the hollow Pd/CeO_2 catalyst treated at 350 and 550 °C, SiO_2 supported Pd NPs calcined at 350 °C, and hollow CeO_2 treated at 350 °C. The label of hm- denotes hollow mesoporous. Adapted from Ref. 51. Copyright 2012 Wiley-VCH Verlag.

Entry	Catalyst		t [h]	Conversion [%]
1	Pd@hm-CeO_2[b]	1st cycle	1.5	>99.9
2		2nd cycle	1.5	>99.9
3		3rd cycle	1.5	>99.9
4	Pd/hm-CeO_2[c]		1.5	42.1
5	Pd/CeO_2[d]		1.5	24.5
6	Pd/C		1.5	62.6

[a] Reaction conditions: 0.5 mmol cinnamyl alcohol, 0.004 mmol Pd, 8 mL toluene, $T = 80$ °C, O_2 flow 5 mL min^{-1}. [b] Treated at 550 °C. [c] hm-CeO_2 surface-supported 4.9 nm Pd nanoparticles treated at 550 °C. [d] Pd/CeO_2 prepared by the incipient wetness impregnation method.

Tab. 2 The aerobic oxidation of cinnamyl alcohol to cinnamaldehyde by Pd@hm-CeO_2, Pd/hm-CeO_2, Pd/CeO_2, and Pt/AC catalysts[a]. Adapted from Ref. 51. Copyright 2012 Wiley-VCH Verlag.

In addition to high-temperature gas phase catalytic reactions, hollow ceria-noble metal composites exhibit structural advantages also in lower-temperature photocatalytic reactions (Table 3). For example, during the photocatalytic reduction of substituted aromatic nitro compounds, the ceria shell acted as the primary active component, which was excited to give photogenerated electron-hole pairs under visible light irradiation, while the encapsulated Pd NPs with a low lying Fermi level served as an electron reservoir to prolong the lifetime of the charge carriers.[62] Of particular interest is that the three-dimensional interfacial contact between Pd cores and ceria shells facilitated efficient charge carrier transfer, thereby leading to the extended lifetime of photogenerated electrons and holes from ceria under visible-light irradiation. This was supported by photoluminescence (PL) analysis (Fig. 18), where the PL intensity of the core-shell Pd@CeO_2 was much weaker than that of supported Pd/CeO_2 and commercial CeO_2, indicative of the efficiently prolonged lifetime of electron-hole pairs in Pd@CeO_2. In addition, CeO_2-Pd hollow nanocomposites exhibited a much better light absorption capability than solid CeO_2 supported Pd NP composite because the hollow structure of the former system allowed more efficient, permeable absorption and scattering of visible light, thereby contributing to photoactivity enhancement.[62]

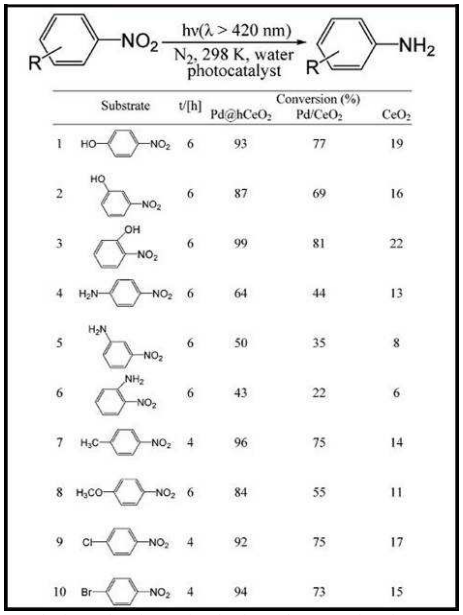

	Substrate	t/[h]	Conversion (%) Pd@hCeO2	Pd/CeO2	CeO2
1	HO–C6H4–NO2	6	93	77	19
2	HO–C6H4–NO2	6	87	69	16
3	OH–C6H4–NO2	6	99	81	22
4	H2N–C6H4–NO2	6	64	44	13
5	H2N–C6H4–NO2	6	50	35	8
6	NH2–C6H4–NO2	6	43	22	6
7	H3C–C6H4–NO2	4	96	75	14
8	H3CO–C6H4–NO2	6	84	55	11
9	Cl–C6H4–NO2	4	92	75	17
10	Br–C6H4–NO2	4	94	73	15

Tab. 3 Photocatalytic reduction of substituted aromatic nitro compounds

over Pd@h CeO_2 core-shell nanocomposite, supported Pd/CeO_2, and commercial CeO_2 aqueous suspension under visible-light irradiation (λ > 420 nm) with the addition of ammonium oxalate as quencher for photogenerated holes and N_2 purge at room temperature. Reprinted from Ref. 62. Copyright 2013 American Chemical Society.

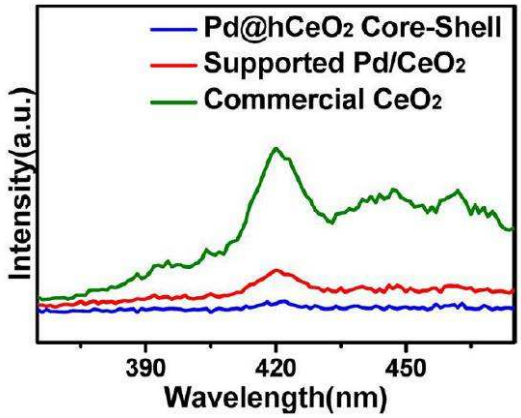

Fig. 18 PL spectra of commercial CeO_2, supported Pd/CeO_2, and Pd@hCeO_2 core-shell nanocomposites. Adapted from Ref. 62. Copyright 2013 American Chemical Society.

4.2 Hollow ceria-metal oxide composites

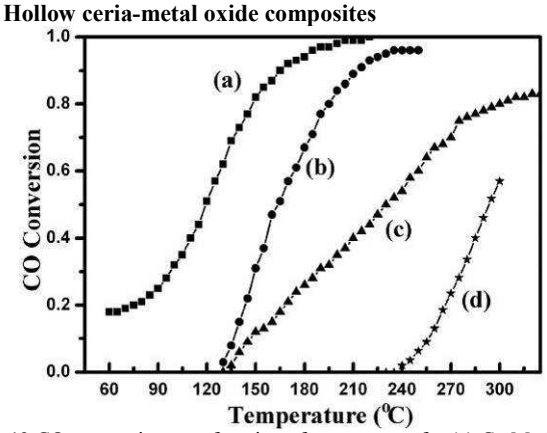

Fig. 19 CO conversion as a function of temperature for (a) Ce-Mn binary oxide NTs; (b) MnO_2; (c) physical mixture of MnO_2 and CeO_2 and (d) CeO_2. Reprinted from Ref. 78. Copyright 2012 Wiley-VCH Verlag.

As stated above, the properties of the composites made of ceria and a secondary metal oxide cannot be simply considered as the sum of the two individual components. Rather, in some cases, they can be more complex and superior in certain aspects due to strong synergistic interactions between the closely packed structural units. For example, Ce-Mn binary oxide NTs exhibited high catalytic activity towards CO oxidation in comparison with both commercially available ceria and manganese oxide particles and their physical mixture (Fig. 19).[78] Specifically, 50% CO conversion was realized at 120 °C with the presence of the Ce-Mn binary oxide NTs, in clear contrast to 165 °C with manganese oxide, 295 °C with ceria and 235 °C with the physical mixture of manganese oxide and ceria particles. It was proposed that due to the multiple valence states of Mn, the active sites of manganese oxide provide oxygen species while ceria stores and releases oxygen via the transformation between Ce^{4+} and Ce^{3+}. During the CO oxidation process, oxygen atoms transfer from O_2 to the active sites of manganese oxide through the oxygen reservoir of ceria that is in close contact with manganese oxide. This greatly increases oxygen mobility on the Ce-Mn binary oxide surface as well as effectively activates molecular oxygen, resulting in high catalytic activity. Therefore, the extremely homogeneous distribution of manganese oxide and ceria throughout the Ce-Mn binary oxide NT wall strengthens this kind of interactions, which is likely responsible for the much higher catalytic activity of the hybrid NTs as compared with the physical mixture of constituent components. In addition, the high specific surface area (~202 m^2/g) of Ce-Mn binary oxide NTs enabled the better contact of catalytically active particles with the gas molecules due to the existence of the interior space and penetrable wall, which was also beneficial for gas-phase reactions.[78] The interaction between ceria and CuO was also demonstrated where the largest exposed ceria-CuO interface in different hollow ceria/CuO composites is considered most catalytically active in CO oxidation.[74]

5. Conclusions and outlook

In this feature article, we described template-engaged synthetic approaches towards various hollow ceria-based composites and the unique advantages of this kind of structures in catalytic reactions. Although tremendous advances have been made in the synthesis of hollow ceria-based composites, several key issues still need to be addressed. For the synthesis of hollow ceria-noble metal composites, (1) tedious and complicated steps are often involved in the hard-template engaged method, including template surface modifications, preparation of noble metal NPs, and complete removal of templates; (2) the noble metal NPs are prone to sintering, especially for those composites where more than one noble metal NPs is simultaneously encapsulated in one hollow ceria particle; (3) current synthetic strategies are generally not applicable for the synthesis of highly stable noble metal NPs with a size of less than 10 nm, which is disadvantageous to the study of size-dependent catalytic reactions; (4) the ceria shell thickness and/or porosity need to be better controlled and optimized. If the ceria shell is too thick or too compact, the reactants are difficult to diffuse through the shell to contact with encapsulated noble metal NPs, resulting in inferior catalytic activities; and (5) correlations between the catalytic activities and the degree of contact between ceria and noble metal NPs have rarely been explored and remain to be established. Regarding the synthesis of hollow ceria-metal oxide composites, (1) the existing hollow ceria-metal oxide composites are mainly in the micro-size range and the synthetic strategies for more promising nano-sized composites need to be further illustrated; (2) the identification and development of novel, new templates, like Cu_2O and $Ce(OH)CO_3$, are highly desirable for the purpose of expanding the scope of ceria-based binary metal oxides that can be prepared. The exploration for a broad range of appropriate templates is still a challenge; (3) the interaction between ceria and secondary metal oxide requires detailed characterizations and in-depth analysis to provide meaningful physical insights, and (4) structural collapse at high temperature also represents a major drawback for most hollow ceria-based composites.

To address the above challenges, some aspects should be more carefully evaluated in future work. (1) It is extremely important to develop new synthetic approaches to construct hollow ceria composites, in which structural parameters such as shell thickness and porosity can be well tuned. In addition, the template-free methods for the synthesis of hollow ceria-based composites are also promising since the template removal at elevated temperature or by strong acid/base erosion is avoided in these methods.[86-88] (2) the combination of characterization and theoretical calculations is highly desirable towards a fundamental understand of the interaction between ceria and noble metal NPs or secondary metal oxides in catalytic reactions; (3) the noble

metal NPs in hollow composites can be extended to noble-metal based bimetallic NPs, where relatively cheap metals are involved, in the form of core@shell or alloy. This kind of architecture not only dramatically lowers the cost of catalysts by decreasing the use of noble metals, but also prompts a possible synergistic effect in catalytic reactions; and (4) novel precursors that simultaneously contain Ce and secondary metal, *e.g.* Metal-Organic Frameworks (MOF), may be good template candidates for the synthesis of hollow ceria/metal oxide composites. Currently, our experiments with such composites are geared towards these objectives. (5) To improve the thermal stability of the hollow ceria-based composites, the ceria can be doped by other species, *e.g.* lanthanum, or zirconium oxide. Overall, although the synthesis and catalytic performance studies regarding the hollow ceria-based composites are still in their infancy, their advantages in catalytic reactions are already apparent. They are expected to become a new generation of high-performance catalysts in terms of high activity, excellent selectivity and long-term stability and hold high potential for industrial applications.

Acknowlegements

We are grateful to NSERC (Discovery grants to D. M. and F. R.) and FQRNT (team grants to D. M. and F. R.) for financial support. F. R. and D. M. also thank MDEIE for an international collaboration grant with the European Network "WIROX". F.R. also acknowledges NSERC for an EWR Steacie Memorial Fellowship.

Notes and references

[a] *School of Chemistry and Chemical Engineering, University of Jinan, 336 Nanxinzhuang West Road, Jinan, Shandong, 250022, China. E-mail: chm_chengz@ujn.edu.cn.*

[b] *Institut National de la Recherche Scientifique (INRS), 1650 Boulevard Lionel-Boulet, Varennes, Québec J3X 1S2, Canada. Fax: 1-450-929-8102; Tel: 1-514-228-6920; E-mail: rosei@emt.inrs.ca;ma@emt.inrs.ca.*

1 H.-P. Liang, H.-M. Zhang, J.-S. Hu, Y.-G. Guo, L.-J. Wan and C.-L. Bai, *Angew. Chem. Int. Ed.*, 2004, **43**, 1540.
2 K. Cheng, S. Peng, C. Xu and S. Sun, *J. Am. Chem. Soc.*, 2009, **131**, 10637.
3 Y. Xia and Z. Tang, *Adv. Funct. Mater.*, 2012, **22**, 2437.
4 X. W. Lou, L. A. Archer and Z. Yang, *Adv. Mater.*, 2008, **20**, 3987.
5 H. C. Zeng, *J. Mater. Chem.*, 2006, **16**, 649.
6 D. Zhang, X. Du, L. Shi and R. Gao, *Dalton Trans.*, 2012, **41**, 14455.
7 X Song, L. Gao and S. Mathur, *J. Phys. Chem. C*, 2011, **115**, 21730.
8 J. Liu, S. Z. Qiao, J. S. Chen, X. W. Lou, X. Xing and G. Q. Lu, *Chem. Commun.*, 2011, **47**, 12578.
9 Y. Chen, H. Chen, D. Zeng, Y. Tian, F. Chen, J. Feng and J. Shi, *ACS Nano*, 2010, **4**, 6001.
10 Q. Li, J. Sheng, Q. Wei, Q. An, X. Wei, P. Zhang and L. Mai, *Nanoscale*, 2014, **6**, 11072.
11 J. Qi, K. Zhao, G. Li, Y. Gao, H. Zhao, R. Yu and Z. Tang, *Nanoscale*, 2014, **6**, 4072.
12 S. Sun and Z. Yang, *Chem. Commun.*, 2014, **50**, 7403.
13 X. Xia, Q. Xiong, Y. Zhang, J. Tu, C. F. Ng and H. J. Fan, *Small*, 2014, **10**, 2419.
14 Z. Zhang, Y. Chen, X. Xu, J. Zhang, G. Xiang, W. He and X. Wang, *Angew. Chem. Int. Ed.*, 2014, **53**, 429.
15 X. Huang, C. Tan, Z. Yin and H. Zhang, *Adv. Mater.*, 2014, **26**, 2185.
16 J. Nai, Y. Tian, X. Guan and L. Guo, *J. Am. Chem. Soc.*, 2013, **135**, 16082.
17 Y. Vasquez, A. K. Sra and R. E. Schaak, *J. Am. Chem. Soc.*, 2005, **127**, 12504.
18 C. Yan and F. Rosei, *New J. Chem.*, 2014, **38**, 1883.
19 H.-W. Liang, S. Liu and S.-H. Yu, *Adv. Mater.*, 2010, **22**, 3925.
20 X. Xia, Y. Wang, A. Ruditskiy and Y. Xia, *Adv. Mater.*, 2013, **25**, 6313.
21 Y. Liu, J. Goebl and Y. Yin, *Chem. Soc. Rev.*, 2013, **42**, 2610.
22 J. Hu, M. Chen, X. Fang and L. Wu, *Chem. Soc. Rev.*, 2011, **40**, 5472.
23 B. D. Anderson and J. B. Tracy, *Nanoscale*, 2014, **6**, 12195.
24 J. Gao, Q. Li, H. Zhao, L. Li, C. Liu, Q. Gong and L. Qi, *Chem. Mater.*, 2008, **20**, 6263.
25 J.-J. Miao, L.-P. Jiang, C. Liu, J.-M. Zhu and J.-J. Zhu, *Inorg. Chem.*, 2007, **46**, 5673.
26 X. Xia, Y. Zhang, D. Chao, C. Guan, Y. Zhang, L. Li, X. Ge, I. M. Bacho, J. Tu and H. J. Fan, *Nanoscale*, 2014, **6**, 5008.
27 C. Sun, H. Li and L. Chen, *Energy Environ. Sci.*, 2012, **5**, 8475.
28 L. Adijanto, D. A. Bennett, C. Chen, A. S. Yu, M. Cargnello, P. Fornasiero, R. J. Gorte and J. M. Vohs, *Nano Lett.*, 2013, **13**, 2252.
29 H.-P. Zhou, H.-S. Wu, J. Shen, A.-X. Yin, L.-D. Sun and C.-H. Yan, *J. Am. Chem. Soc.*, 2010, **132**, 4998.
30 M. Cargnello, N. L. Wieder, T. Montini, R. J. Gorte and P. Fornasiero, *J. Am. Chem. Soc.*, 2010, **132**, 1402.
31 T. Kayama, K. Yamazaki and H. Shinjoh, *J. Am. Chem. Soc.*, 2010, **132**, 13154.
32 J. Zhang, L. Li, X. Huang and G. Li, *J. Mater. Chem.*, 2012, **22**, 10480.
33 H. Li, G. Qi, Tana, X. Zhang, X. Huang, W. Li and W. Shen, *Appl. Catal. B: Environ.*, 2011, **103**, 54.
34 S. Y. Yao, W. Q. Xu, A. C. Johnston-Peck, F. Z. Zhao, Z. Y. Liu, S. Luo, S. D. Senanayake, A. Martínez-Arias, W. J. Liu and J. A. Rodriguez, *Phys. Chem. Chem. Phys.*, 2014, **16**, 17183.
35 N. Qiu, J. Zhang and Z. Wu, *Phys. Chem. Chem. Phys.*, 2014, **16**, 22659.
36 P. Singha and M. S. Hegde, *Dalton Trans.*, 2010, **39**, 10768.
37 Y. Li and W. Shen, *Chem. Soc. Rev.*, 2014, **43**, 1543.
38 N. Yi, R. Si, H. Saltsburg and M. F.-Stephanopoulos, *Energy Environ. Sci.*, 2010, **3**, 831.
39 N. Acerbi, S. C. E. Tsang, G. Jones, S. Golunski and P. Collier, *Angew. Chem. Int. Ed.*, 2013, **52**, 7737.
40 X.-S. Huang, H. Sun, L.-C. Wang, Y.-M. Liu, K.-N. Fan and Y. Cao, *Appl. Catal. B: Environ.*, 2009, **90**, 224.
41 J. A. Rodriguez, R. Si, J. Evans, W. Xu, J. C. Hanson, J. Tao and Y. Zhu, *Catal. Today*, 2015, **240**, 229.
42 H. Y. Kim, H. M. Lee and G. Henkelman, *J. Am. Chem. Soc.*, 2012, **134**, 1560.
43 N. Ta, J. Liu, S. Chenna, P. A. Crozier, Y. Li, A. Chen and W. Shen, *J. Am. Chem. Soc.*, 2012, **134**, 20585.
44 P. Xu, R. Yu, H. Ren, L. Zong, J. Chen and X. Xing, *Chem. Sci.*, 2014, **5**, 4221.
45 J. Zhang, G. Chen, M. Chaker, F. Rosei and D. Ma, *Appl. Catal. B: Environ.*, 2013, **132-133**, 107.
46 B. Liu, Q. Wang, S. Yu, T. Zhao, J. Han, P. Jing, W. Hu, L. Liu, J. Zhang, L.-D. Sun and C.-H. Yan, *Nanoscale*, 2013, **5**, 9747.
47 C. Wen, Y. Zhu, Y. Ye, S. Zhang, F. Cheng, Y. Liu, P. Wang and F. Tao, *ACS Nano*, 2012, **6**, 9305.
48 K. An, S. Alayoglu, N. Musselwhite, S. Plamthottam, G. Melaet, A. E. Lindeman and G. A. Somorjai, *J. Am. Chem. Soc.*, 2013, **135**, 16689.
49 P. Concepción, A. Corma, J. S.-Albero, V. Franco and J. Y. C.-Ching, *J. Am. Chem. Soc.*, 2004, **126**, 5523.
50 C.-M. Fan, L.-F. Zhang, S.-S. Wang, D.-H. Wang, L.-Q. Lu and A.-W. Xu, *Nanoscale*, 2012, **4**, 6835.
51 C. Chen, X. Fang, B. Wu, L. Huang and N. Zheng, *ChemCatChem.*, 2012, **4**, 1578.
52 N. C. Strandwitz and G. D. Stucky, *Chem. Mater.*, 2009, **21**, 4577.
53 X. Lai, J. E. Halpert and D. Wang, *Energy Environ. Sci.*, 2012, **5**, 5604.
54 M.-M. Titirici, M. Antonietti and A. Thomas, *Chem. Mater.*, 2006, **18**, 3808.
55 Y. Chen and J. Lu, *J. Porous. Mater.*, 2012, **19**, 289.
56 L-S. Zhang, L.-Y. Jiang, C.-Q. Chen, W. Li, W.-G. Song and Y.-G. Guo, *Chem. Mater.*, 2010, **22**, 414.
57 D. G. Shchukin and R. A. Caruso, *Chem. Mater.*, 2004, **16**, 2287.
58 D. Zhang, C. Pan, L. Shi, L. Huang, J. Fang, H. Fu, *Microporous Mesoporous Mater.*, 2009, **117**, 193.
59 D. Zhang, H. Fu, L. Shi, J. Fang, Q. Li, *J. Solid State Chem.*, 2007, **180**, 654.

60 Y. Sun, L. Zhang, Y. Wang, P. Chen, S. Xin, H. Jiu and J. Liu, *J. Alloys Compd.*, 2014, **586**, 441.
61 B. Liu, S. Yu, Q. Wang, W. Hu, P. Jing, Y. Liu, W. Jia, Y. Liu, L. Liu and J. Zhang, *Chem. Commun.*, 2013, **49**, 3757.
62 N. Zhang and Y.-J. Xu, *Chem. Mater.*, 2013, **25**, 1979.
63 K. Yoon, Y. Yang, P. Lu, D. Wan, H.-C. Peng, K. S. Masias, P. T. Fanson, C. T. Campbell and Y. Xia, *Angew. Chem. Int. Ed.*, 2012, **51**, 9543.
64 C. Yuan, H. B. Wu, Y. Xie and X. W. Lou, *Angew. Chem. Int. Ed.*, 2013, **52**, 2.
65 Q. Xie, Y. Zhao, H. Guo, A. Lu, X. Zhang, L. Wang, M.-S. Chen and D.-L. Peng, *ACS Appl. Mater. Interfaces*, 2014, **6**, 421.
66 H. Jiang, J. Zhao, D. Jiang and M. Zhang, *Catal Lett.*, 2014, **144**, 325.
67 P. Bocchetta, M. Santamaria and F. D. Quarto, *Electrochem. Solid-State Lett.*, 2008, **11**, K27.
68 R. O. Fuentes, L. M. Acuňa, M. G. Zimicz, D. G. Lamas, J. G. Sacanell, A. G. Leyva and R. T. Baker, *Chem. Mater.*, 2008, **20**, 7356.
69 L. Xu, H. Song, B. Dong, Y. Wang, J. Chen and X. Bai, *Inorg. Chem.*, 2010, **49**, 10590.
70 L. M. Acuňa, F. F. Muňoz, M. D. Cabezas, D. G. Lamas, G. Leyva, M. C. A. Fantini, R. T. Baker and R. O. Fuentes, *J. Phys. Chem. C*, 2010, **114**, 19687.
71 P. Song, Q. Wang and Z. Yang, *Sens. Actuators, B*, 2012, **173**, 839.
72 G. M.-Galicia, R. P. -Hernández, C. E. G.-Wing and D. M.-Anaya, *Phys. Chem. Chem. Phys.*, 2011, **13**, 16756.
73 C. Jin, X. Cao, F. Lu, Z. Yang and R. Yang, *ACS Appl. Mater. Interfaces*, 2014, **6**, 847.
74 H. Bao, Z. Zhang, Q. Hua and W. Huang, *Langmuir*, 2014, **30**, 6427.
75 X. Liang, X. Wang, Y. Zhuang, B. Xu, S. Kuang and Y. Li, *J. Am. Chem. Soc.*, 2008, **130**, 2736.
76 J. Zhang, L. Li, X. Huang and G. Li, *J. Mater. Chem.*, 2012, **22**, 10480.
77 F. Zhu, G. Chen, S. Sun and X. Sun, *J. Mater. Chem. A*, 2013, **1**, 288.
78 G. Chen, F. Rosei and D. Ma, *Adv. Funct. Mater.*, 2012, **22**, 3914.
79 G. Chen, C. Xu, X. Song, W. Zhao and Y. Ding, *Inorg. Chem.*, 2008, **47**, 723.
80 G. Chen, G. S. Sun, X. Sun, W. Fan and T. You, *Inorg. Chem.*, 2009, **48**, 1334.
81 Y.-J. Feng, L.-L. Liu and X.-D. Wang, *J. Mater. Chem.*, 2011, **21**, 15442.
82 J. Qi, J. Chen, G. Li, S. Li, Y. Gao and Z. Tang, *Energy Environ. Sci.*, 2012, **5**, 8937.
83 Z. Shen, J. Liu, F. Hu, S. Liu, N. Cao, Y. Sui, Q. Zeng and Y. Shen, *CrystEngComm.*, 2014, **16**, 3387.
84 H. Guo, Y. He, Y. Wang, L. Liu, X. Yang, S. Wang, Z. Huang and Q. Wei, *J. Mater. Chem. A*, 2013, **1**, 7494.
85 X. Wang, D. Liu, S. Song and H. Zhang, *J. Am. Chem. Soc.*, 2013, **135**, 15864.
86 C.-Y. Cao, Z.-M. Cui, C.-Q. Chen, W.-G. Song and W. Cai, *J. Phys. Chem. C*, 2010, **114**, 9865.
87 G. Chen, F. Zhu, X. Sun, S. Sun and R. Chen, *CrystEngComm*., 2011, **13**, 2904.
88 G. Chen, C. Xu, X. Song, S. Xu, Y. Ding and S. Sun, *Cryst. Growth & Des.*, 2008, **8**, 4449.

Guozhu Chen is currently an Associate Professor at University of Jinan, China. He received his Ph.D. degree in Inorganic Chemistry in 2009 from Shandong University, China. After graduation, he joined Prof. Ma's group at Institut National de la Recherche Scientifique, Canada, as a postdoctoral fellow. His main research interest is the rational synthesis of functional nanomaterials, including bimetallic nanoparticles, hollow structured metal oxides and metal nanoparticle/metal oxide nanocomposites, for heterogeneous catalysis (e.g., CO oxidation and dehydrogenation).

Federico Rosei has held the Canada Research Chair in Nanostructured Organic and Inorganic Materials between 2003 and 2013, and is Professor and Director of the Energy, Materials and Telecommunications Centre of INRS in Varennes (QC) Canada. Since January 2014, he holds the UNESCO Chair in Materials and Technologies for Energy Conversion, Saving and Storage. He obtained his PhD in 2001 from the University of Rome ''La Sapienza'' (Italy). He is Fellow of the Royal Society of Canada, Member of the European Academy of Sciences, Fellow of the American Physical Society, Fellow of the American Association for the Advancement of Science, Fellow of SPIE, Fellow of the Royal Society of Chemistry (UK), Fellow of the Institute of Physics, Fellow of the Institution of Engineering and Technology, Fellow of the Institute of Materials, Metallurgy and Mining, Fellow of the Institute of Nanotechnology, Senior Member of the IEEE, Fellow of the Engineering Institute of Canada, Member of the Global Young Academy, Fellow of the Australian Institute of Physics and Member of the Sigma Xi Society.

Dongling Ma has been a professor at Institut national de la recherche scientifique, Canada since 2006. Her main research interest consists in the development of various nanomaterials (e.g., semiconductor quantum dots, transition metal nanoparticles, plasmonic nanostructures and nanohybrids) for applications in energy, catalysis and biomedical sectors. She was awarded Natural Sciences and Engineering Research Council Visiting Fellowships and worked at National Research Council of Canada during 2004–2006. She received her Ph.D. in Materials Science & Engineering from Rensselaer Polytechnic Institute, USA in 2004.